

Pan-Trk Immunohistochemistry Identifies *NTRK* Rearrangements in Pediatric Mesenchymal Tumors

Erin R. Rudzinski, MD,* Christina M. Lockwood, PhD,† Bradley A. Stohr, MD, PhD,‡ Sara O. Vargas, MD,§ Rachel Sheridan, MD,|| Jennifer O. Black, MD,¶ Veena Rajaram, MD,# Theodore W. Laetsch, MD,** and Jessica L. Davis, MD,††

Abstract: Activating neurotrophic receptor kinase (*NTRK*) fusions define certain pediatric mesenchymal tumors, including infantile fibrosarcoma and cellular mesoblastic nephroma. Traditionally, molecular confirmation of these fusions has included either fluorescent in situ hybridization for *ETV6* rearrangements or reverse-transcriptase polymerase chain reaction for the classic *ETV6-NTRK3* fusion. However, these methods overlook variant *NTRK* rearrangements, which are increasingly appreciated as recurrent events in a subset of pediatric mesenchymal tumors. New therapeutic agents successfully target these fusions and may prevent morbid surgeries in very young children, making recognition of tumors harboring *NTRK* rearrangements of increasing importance. We evaluated the performance of immunohistochemical (IHC) staining using pan-Trk and TrkA antibodies in 79 pediatric mesenchymal tumors. Negative controls included pediatric mesenchymal tumors not harboring ($n=28$) or not expected to harbor ($n=22$) *NTRK* fusions. *NTRK* rearrangements were detected predominantly by DNA-based next-generation sequencing assays, specifically UW OncoPlex and UCSF500 Cancer Gene Panel. Pan-Trk IHC (EPR17341) was 97% sensitive and 98% specific for the presence of an *NTRK* rearrangement, and TrkA IHC (EP1058Y) was 100% sensitive and 63% specific for the presence of an *NTRK* rearrangement. Tumors with *NTRK1* or *NTRK2* rearrangements showed cytoplasmic staining, whereas tumors with *NTRK3* rearrangements showed nuclear +/- cytoplasmic staining. We conclude that pan-Trk IHC is a highly sensitive and specific marker for *NTRK* rearrangements in pediatric mesenchymal tumors.

Key Words: *NTRK*, Trk, immunohistochemistry, soft tissue sarcoma, pediatric

(*Am J Surg Pathol* 2018;42:927–935)

From the *Department of Laboratories, Seattle Children's Hospital; †Department of Laboratory Medicine, University of Washington Medical Center, Seattle, WA; ‡Department of Pathology, University of California San Francisco, San Francisco, CA; §Department of Pathology, Boston Children's Hospital, Boston, MA; ||Department of Pathology, Cincinnati Children's Hospital, Cincinnati, OH; ¶Department of Pathology, Children's Hospital Colorado, Aurora, CO; #Department of Pathology; **Department of Pediatrics and Simmons Comprehensive Cancer Center, University of Texas, Southwestern and Children's Health, Dallas, TX; and ††Department of Pathology, Oregon Health and Science University, Portland, OR.

Conflicts of Interest and Source of Funding: The authors have disclosed that they have no significant relationships with, or financial interest in, any commercial companies pertaining to this article.

Correspondence: Erin R. Rudzinski, MD, Department of Laboratories, Seattle Children's Hospital, OC.8.720, 4800 Sandpoint Way NE, Seattle, WA 98105 (e-mail: erin.rudzinski@seattlechildrens.org). Copyright © 2018 Wolters Kluwer Health, Inc. All rights reserved.

Neurotrophic tyrosine kinase receptor genes neurotrophic receptor kinase 1 (*NTRK1*), *NTRK2*, and *NTRK3* encode 3 corresponding proteins, tropomyosin receptor kinases (Trk) A, B, and C, respectively. Oncogenic fusions involving the kinase domain of *NTRK1*, *NTRK2*, or *NTRK3* are present in a wide variety of cancer types.¹ These fusions are over-represented in pediatric tumors, particularly in pediatric mesenchymal tumors including the well-recognized *ETV6-NTRK3* fusions that are the driving mutation in infantile fibrosarcoma and cellular congenital mesoblastic nephroma.^{2,3} In addition, variant *NTRK* rearrangements are increasingly recognized as recurrent events in a subset of pediatric mesenchymal tumors.^{4–8}

Many pediatric *NTRK*-rearranged mesenchymal tumors present as large, infiltrative masses which necessitate neoadjuvant chemotherapy and/or require potentially morbid resections in very young children. However, there are now therapeutic agents, including Larotrectinib and Ertrectinib, directed specifically against TrkA, TrkB, and TrkC.^{1,9–12} Recent studies have shown excellent activity to larotrectinib in pediatric patients with *NTRK*-rearranged tumors.^{13,14} Thus, early recognition of these translocations is of increasing importance.

Screening for *NTRK* fusions can be done on a molecular basis by a variety of techniques including next-generation sequencing (NGS) of DNA or RNA. However, molecular tests remain relatively expensive and time-consuming, and are not immediately available in many institutions, thus potentially delaying use of Trk inhibitor therapy. In addition, these assays are subject to sampling error or sample degradation, and the false negative rate of individual molecular tests is often unclear. In contrast, immunohistochemistry (IHC) offers the advantage of increased speed, wide availability and cost-savings with superior histologic correlation. The goal of this study was to determine the performance characteristics of IHC for antibodies against Trk proteins as a surrogate marker of *NTRK* gene fusion status in pediatric mesenchymal tumors.

MATERIALS AND METHODS

Case Selection

The study was conducted with the approval of all local institutional review boards. Patients with diagnoses of infantile fibrosarcoma or congenital cellular mesoblastic nephroma, or for which these were considered in the differential diagnosis, were identified from the pathology

databases at Seattle Children’s Hospital and University of California San Francisco. Cases of infantile fibrosarcoma or cellular mesoblastic nephroma with confirmed *ETV6* break-apart by fluorescent in situ hybridization (FISH) or *ETV6-NTRK3* fusions by reverse-transcriptase polymerase chain reaction (RT-PCR) were not sequenced (n = 7), but the remaining cases were submitted for NGS (n = 49). Four additional patients with confirmed *NTRK* rearrangements were contributed by other institutions.

Another group of 22 miscellaneous soft tissue tumors, which were well-defined histologically were also used as a negative control group; none of these tumors were expected to harbor *NTRK* rearrangements based on the histologic diagnosis. This validation cohort included: 2 dermatofibrosarcoma protuberans (with confirmed *PDGFB* rearrangements), 2 classic myofibromas, 4 desmoid tumors, 1 malignant peripheral nerve sheath tumor, 2 synovial sarcomas (with confirmed *SYT* rearrangements), 1 spindle cell rhabdomyosarcoma, 1 clear cell sarcoma of the kidney, 1 CCNB3 positive sarcoma, 4 ALK-positive inflammatory myofibroblastic tumors, 1 nodular fasciitis, 2 schwannomas, and 1 neurofibroma.

Next-generation Sequencing

Cases were sequenced by various clinically validated NGS platforms performed in CLIA-approved laboratories. Thirty-six total cases were sequenced using UW OncoPlex, a targeted DNA-based platform that includes *NTRK1*, *NTRK2*, and *NTRK3*. Seventeen cases were sequenced using UCSF500 Cancer Gene Panel, which is also a targeted DNA-based platform that includes *NTRK1*, *NTRK2*, and *NTRK3*. Four patients were sequenced by both panels. Four additional cases submitted by other institutions; 3 were sequenced by platforms chosen locally, and 1 was confirmed by *ETV6* FISH.

Both UW OncoPlex and UCSF500 have probes for exons and select introns of *NTRK1*, *NTRK2*, and *NTRK3* to detect rearrangements. Additional probes for *ETV6* exons and select introns are included to detect *ETV6-NTRK3* fusions, and UW OncoPlex includes additional probes for select exons and introns of *EML4* to detect *EML4-NTRK3* rearrangements. These tests do not include all introns affected by *NTRK* rearrangements due to the size and use of a DNA-based capture approach.

TABLE 1. Pan-Trk and TrkA IHC Characteristics for *NTRK*-rearranged Mesenchymal Tumors

Case	Site	NTRK Gene	Partner Gene	Staining Pattern			
				Pan-Trk		TrkA	
				Cytoplasmic	Nuclear	Cytoplasmic	Nuclear
1	ST	<i>NTRK1</i> intron 8	<i>TPM3</i> intron 7	+++	–	+++	–
2	ST	<i>NTRK1</i> intron 8	<i>TPM3</i> intron 7	+++	–	+++	–
3	ST	<i>NTRK1</i> intron 8	<i>TPM3</i> intron 7	+++	–	+++	–
4	ST	<i>NTRK1</i> intron 8	<i>TPM3</i> intron 7	++	–	+++	–
5	ST	<i>NTRK1</i> intron 8	<i>TPM3</i> intron 7	+++	–	+++	–
6	ST	<i>NTRK1</i>	<i>TPM3</i>	+++	–	ND	ND
7	ST (gastric)	<i>NTRK1</i> intron 8	<i>TPM3</i> intron 7	+++	–	ND	ND
8	ST	<i>NTRK1</i> intron 10	<i>LMNA</i> intron 3	++	–	+++	–
9	ST	<i>NTRK1</i> intron 9	<i>LMNA</i> intron 3	+++	–	+++	–
10	ST	<i>NTRK1</i> intron 10	<i>MIR548F1</i> exon 9	++	–	++	–
11	ST	<i>NTRK1</i>	<i>SQSTM1</i>	+++	–	+++	–
12	ST	<i>NTRK1</i> intron 10	<i>TPR</i> intron 20	++	–	++	–
13	ST	<i>NTRK1</i> partial amplification (exons 7-17)	–	+	–	++	–
14	ST	<i>NTRK2</i> exon 4	<i>STRN</i> exon 15	++	–	++, Dot	–
15	ST	<i>NTRK3</i> intron 13	<i>EML4</i> intron 2	+	+	+, Dot	+
16	ST	<i>NTRK3</i> intron 13	<i>ETV6</i> intron 5	+	+++	++, Dot	++
17*	ST	<i>NTRK3</i> intron 14, intron 14†	<i>ETV6</i> intron 5, intron 5†	++	++	++	++
18*	ST	<i>NTRK3</i> intron 13	<i>ETV6</i> intron 5	+	+	++	+
19*	ST	<i>NTRK3</i> intron 14, intron 13	<i>ETV6</i> intron 5, intron 7	+	+	+, Dot	+
20*	ST	<i>NTRK3</i> intron 13	<i>ETV6</i> intron 5	+	+	+	–
21	ST (dura)	<i>NTRK3</i>	<i>ETV6</i>	+	++	ND	ND
22	ST	<i>NTRK3</i> intron 14	<i>ETV6</i> intron 5	+	++	++, Dot	+
23	ST		<i>ETV6+</i>	+	+	++, Dot	–
24	ST		<i>ETV6+</i>	–	+	++, Dot	–
25	ST		<i>ETV6+</i>	–	+	++	+
26	ST		<i>ETV6+</i>	+	++	++	++
27	ST		<i>ETV6+</i>	–	+	++	–
28*	Renal	<i>NTRK3</i> intron 13	<i>ETV6</i> intron 5	–	–	+++	–
29	Renal		<i>ETV6+</i>	+	+	ND	ND
30	Renal		<i>ETV6+</i>	+	+	++, Dot	–
31	ST	QNS	QNS	–	+	–	+

*Original cytogenetic testing negative for *ETV6-NTRK3* translocation (FISH, RT-PCR, or karyotype).

†Two distinct fusion breakpoints between *ETV6* and *NTRK3* were identified in this case.

FISH indicates fluorescent in situ hybridization; ND, not done; QNS, quantity not sufficient; RT-PCR, reverse-transcriptase polymerase chain reaction; STS, soft tissue.

Immunohistochemistry

IHC staining was performed with an anti-TrkA monoclonal antibody clone EP1058Y (Abcam, Cambridge, MA), which targets residues surrounding tyrosine 791 of human TrkA, as well as with a pan-Trk monoclonal antibody clone EPR17341 (Abcam) which targets an amino

acid sequence 800 to the C-terminus within human TrkA, TrkB, and TrkC. Staining was performed on an automated system (Benchmark ULTRA; Ventana Medical Systems, Tucson, AZ) with the following protocol: anti-TrkA and pan-Trk 1:500 dilution, 32 minutes incubation time at 37°C with standard (high pH) cell conditioning. One case with a

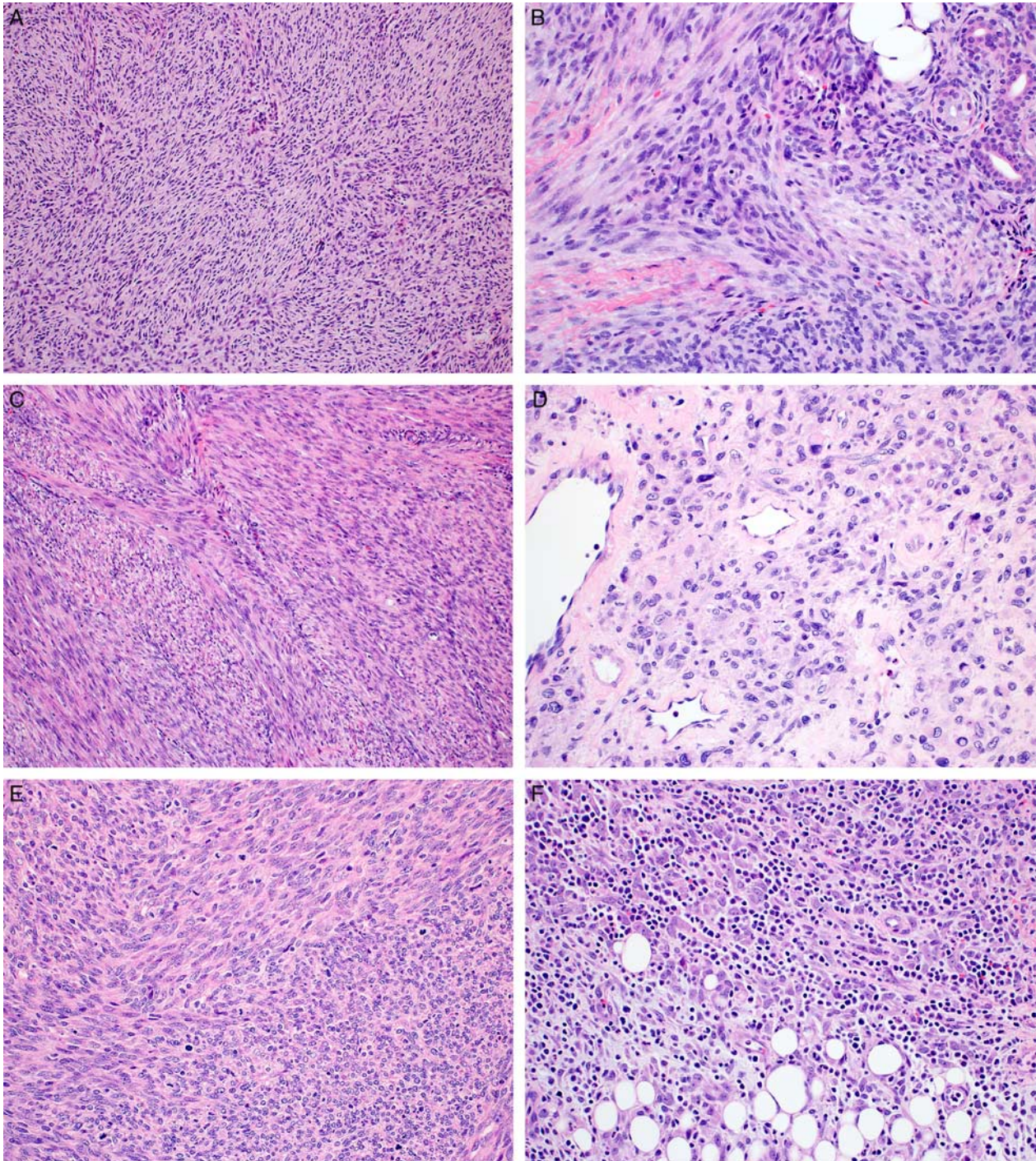


FIGURE 1. Representative H&E images of various cases with a variety of *NTRK* rearrangements include (A) case 9: *LMNA-NTRK1* fusion; (B) case 3: *TPM3-NTRK1* fusion; (C) case 13: *NTRK1* amplification; (D) case 14: *NTRK2-STRN* fusion; (E) case 17: *ETV6-NTRK3* fusion; and (F) case 18: *ETV6-NTRK3* fusion H&E indicates hematoxylin and eosin.

confirmed *TPM3-NTRK1* rearrangement was used as the positive control. Non-neoplastic tissues (skin, blood vessels, inflammatory cells, renal cortical epithelium) were used as negative internal controls.

IHC staining was assessed in both tumor nuclei and cytoplasm and recorded as weak, moderate, or strong. Cytoplasmic staining was required to be diffuse (> 50% of tumor cells) to be scored. Any amount of nuclear staining

was scored. Other patterns, such as perinuclear dot accentuation, were also recorded.

RESULTS

Case Selection and Characteristics

NTRK rearrangements were identified in 19 of cases (6 previously published) submitted for NGS sequencing

TABLE 2. Pan-Trk and TrkA IHC Characteristics for Non-*NTRK*-rearranged Mesenchymal Tumors

Case	Diagnosis	Expected Mutation Detected	Staining Pattern			
			Pan-Trk		TrkA	
			Cytoplasmic	Nuclear	Cytoplasmic	Nuclear
1	DFSP	<i>PDGFB</i>	-	-	-	-
2	DFSP	<i>PDGFB</i>	-	-	Dot	-
3	FHI	<i>EGFR</i> exon 20	-	-	Dot	-
4	FHI	<i>EGFR</i> exon 20	-	-	+, Dot	-
5	FHI	<i>EGFR</i> exon 20	-	-	+	-
6	Lipofibromatosis	None	-	-	-	-
7	Lipoblastomatosis	None	-	-	-	-
8	Myofibroma	ND	-	-	+, Dot	-
9	Myofibroma	ND	-	-	Dot	-
10	Myofibromatosis	<i>PDGFRB</i>	-	-	-	-
11	Cellular myofibroma	None	-	-	+, Dot	-
12	Cellular myofibroma	None	-	-	+	-
13	Cellular myofibroma	None	-	-	+	-
14	Desmoid	<i>APC</i>	-	-	-	-
15	Desmoid	ND	-	-	Dot	-
16	Desmoid	ND	-	-	+	-
17	Desmoid	ND	-	-	+	-
18	Desmoid	ND	-	-	+	-
19	MPNST	<i>NFI</i>	-	-	++	-
20	MPNST	ND	-	-	+	-
21	Synovial sarcoma	<i>SYT</i>	Focal	-	-	-
22	Synovial sarcoma	<i>SYT</i>	Focal	-	+	-
23	Spindle cell RMS	<i>NRAS</i>	-	-	++	-
24	Spindle cell RMS	ND	-	-	Dot	-
25	Nodular fasciitis	ND	-	-	Dot	-
26	Classic schwannoma	ND	-	-	Dot	-
27	Classic schwannoma	ND	-	-	Dot	-
28	Cellular schwannoma	None	-	-	-	-
29	Neurofibroma	ND	-	-	Dot	-
30	IMT	None	-	-	Dot	-
31	IMT	None	-	-	+	-
32	IMT	ALK	-	-	+, Dot	-
33	IMT	ALK	-	-	+, Dot	-
34	IMT	ALK	-	-	+, Dot	-
35	IMT	ALK	-	-	++	-
36	<i>BCOR</i> rearranged sarcoma	<i>CCNB3</i>	-	-	-	-
37	Undifferentiated pleomorphic sarcoma	ND	-	-	-	-
38	High-grade sarcoma	None	-	-	-	-
39	High-grade sarcoma	None	-	-	-	-
40	High-grade sarcoma	None	-	-	-	-
41	High-grade sarcoma	None	-	-	-	-
42	Low-grade spindle cell lesion	None	ND	ND	-	-
43	Low-grade spindle cell lesion	None	+	-	++	-
44	Low-grade spindle cell lesion	None	-	-	-	-
45	Low-grade spindle cell lesion	None	ND	ND	-	-
46	Low-grade spindle cell lesion	None	-	-	-	-
47	Metanephric stromal tumor	<i>BRAF</i> V600E	-	-	-	-
48	Classic mesoblastic nephroma	None	-	-	Dot	-
49	Cellular mesoblastic nephroma	<i>EGFR</i> mutation	-	-	ND	ND
50	Clear cell sarcoma of the kidney	ND	-	-	+, Dot	-

DFSP indicates dermatofibrosarcoma protuberans; FHI, fibrous hamartoma of infancy; IMT, inflammatory myofibroblastic tumor; MPNST, malignant peripheral nerve sheath tumor; ND, not done; RMS, rhabdomyosarcoma.

(Table 1).⁵ These fusions included: *ETV6-NTRK3* (n=8), *EML4-NTRK3* (n=1), *STRN-NTRK2* (n=1), and *NTRK1* with a variety of partners including *TPM3* (n=7), *LMNA* (n=2), *TPR* (n=1), *SQSTM1* (n=1), and 1 novel partner, *MIR548F1*. The following transcript identifiers were used: *NTRK1*: NM_002529; *NTRK2*: NM_006180; *NTRK3*: NM_001012338; *TPM3*: NM_152263; *LMNA*: NM_170707; *TPR*: NM_003292; *ETV6*: NM_001987; *STRN*: NM_003162. One case had partial low-level *NTRK1* amplification involving exons 7 to 17, downstream of an apparent breakpoint in intron 6; however, a fusion partner could not be identified. One case failed sequencing, with insufficient tumor to analyze. Seven cases showed *ETV6* rearrangement by FISH or RT-PCR. Representative hematoxylin and eosin images from 6 cases with confirmed *NTRK* rearrangements are shown in Figure 1.

Twenty-eight cases were sequenced but lacked evidence for an *NTRK* rearrangement (Table 2). These included the following diagnoses: 3 fibrous hamartomas of infancy, 1 lipofibromatosis, 1 lipoblastomatosis, 1 myofibromatosis, 3 cellular myofibromas, 1 desmoid

fibromatosis, 2 ALK-negative inflammatory myofibroblastic tumors, 1 cellular schwannoma, 1 malignant peripheral nerve sheath tumor, 1 spindle cell rhabdomyosarcoma, 1 undifferentiated pleomorphic sarcoma, 1 metanephric stromal tumor, 1 cellular mesoblastic nephroma, 1 classic mesoblastic nephroma, 4 high-grade sarcomas—not otherwise specified (NOS), and 5 low-grade spindle cell lesions—NOS. NGS confirmed other diagnostic alterations in 10 of these cases; no diagnostic alterations were identified by NGS in the other 18 cases.

Immunohistochemistry

Pan-Trk IHC was performed on 79 cases. Twenty-nine of 30 tumors with confirmed *NTRK* rearrangements by NGS were positive for pan-Trk by IHC (Figs. 2–4). Two negatively staining, non-*NTRK*-rearranged cases are shown in Figure 5. One renal mass with a confirmed *ETV6-NTRK3* fusion lacked pan-Trk staining. One low-grade spindle cell tumor, NOS lacking an identified *NTRK* rearrangement by NGS showed weak, cytoplasmic staining with pan-Trk, whereas the other 47 of 48 cases were negative for pan-Trk. This represents a sensitivity of

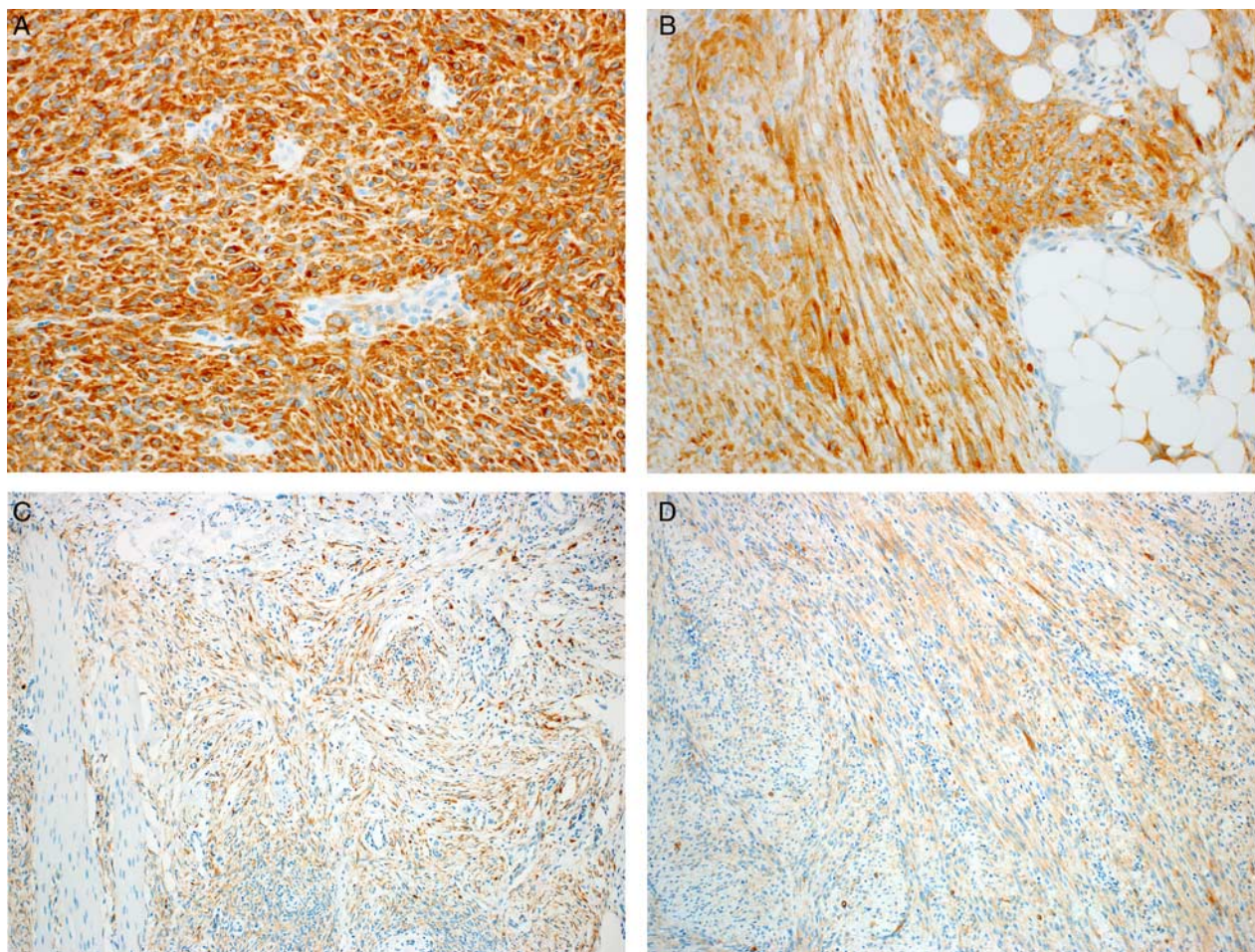


FIGURE 2. *NTRK1* rearrangement. Strong diffuse cytoplasmic staining for pan-Trk was seen in most *NTRK1*-rearranged tumors (A, case 9: *LMNA*; B, case 3: *TPM3*). A few tumors showed moderate (C, case 8: *LMNA*) or weak (D, case 13: *NTRK1* amp) but diffuse cytoplasmic staining.

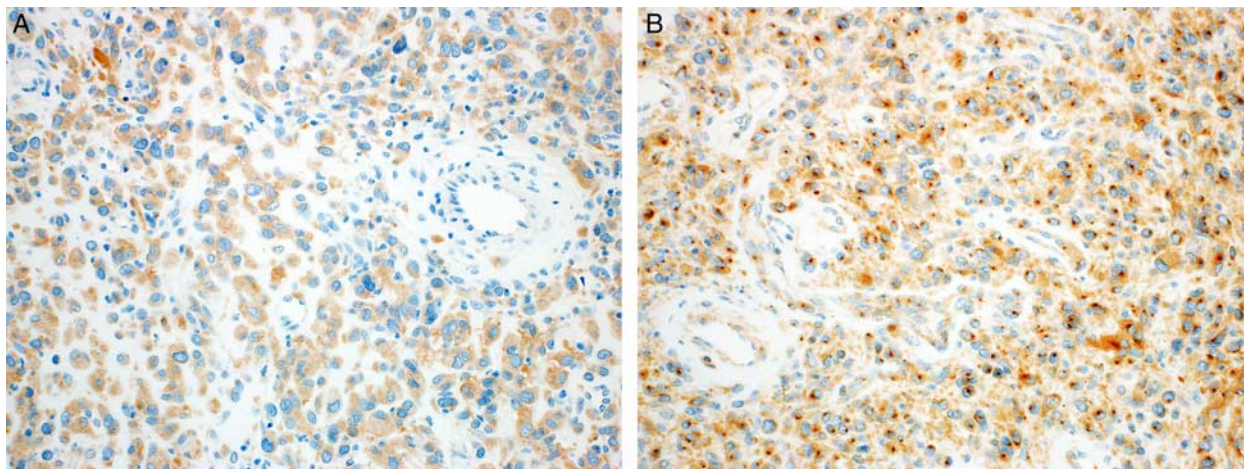


FIGURE 3. *NTRK2* rearrangement. A, Pan-Trk IHC showed diffuse, moderate cytoplasmic staining in 1 case with an *NTRK2-STRN* fusion (case 14). B, TrkA IHC in this same case showed diffuse, moderate cytoplasmic staining with perinuclear dot accentuation (a nonspecific pattern).

96.7%, a specificity of 97.9%, a positive predictive value of 96.67%, and a negative predictive value of 97.9%. Distinct patterns of staining were seen with *NTRK1/NTRK2* versus *NTRK3* rearrangements; *NTRK1/NTRK2* fused cases (Figs. 1, 2) showed only cytoplasmic staining, whereas all IHC positive *NTRK3*-rearranged cases (Fig. 3) showed nuclear +/- cytoplasmic staining. No cases showed membranous or perinuclear staining.

TrkA IHC was performed on 76 cases. Given the similarity of the target region between the pan-Trk and TrkA antibodies, we saw significant cross-reactivity with this antibody for *NTRK1*, *NTRK2*, and *NTRK3* gene rearrangements. Twenty-six of 26 tumors with confirmed *NTRK* rearrangements by NGS were positive for TrkA by IHC. However, 14 of 49 non-*NTRK*-rearranged cases had weak staining and 4 had moderate staining. This represents a sensitivity of 100%, a specificity of 63.3%, a positive predictive value of 59.1%, and a negative predictive value of 100%. A similar relationship between pattern of staining and specific *NTRK* rearrangement was also seen. *NTRK1/NTRK2*-rearranged tumors showed only cytoplasmic staining, whereas 8 of 14 *NTRK3*-rearranged tumors showed nuclear in addition to cytoplasmic staining. Perinuclear dot staining was seen in several cases, including cases lacking *NTRK* rearrangements (Fig. 3B), and this pattern of staining did not correlate with presence of a gene fusion (Table 2). No cases showed cytoplasmic membrane or nuclear membrane staining.

Five of 9 cases with positive IHC staining and confirmed *ETV6-NTRK3* fusions by NGS were negative by the original testing method (2 FISH, 1 RT-PCR, 1 FISH and RT-PCR, 1 karyotype). In addition, IHC for both pan-Trk and TrkA were positive in 1 case which lacked sufficient tumor tissue for NGS analysis.

DISCUSSION

NTRK rearrangements occur frequently in pediatric mesenchymal tumors.⁴⁻⁸ Although conventional molecular

and cytogenetic assays (FISH and RT-PCR) are routinely used in making the diagnosis of infantile fibrosarcoma or congenital cellular mesoblastic nephroma, these methods target only the classic *ETV6-NTRK3* rearrangement. Given the increasing recognition of variant *NTRK* rearrangements in pediatric soft tissue tumors (including infantile fibrosarcoma/cellular mesoblastic nephroma and lipofibromatosis-like neural tumor), and the subsequent treatment implications for patients with aggressive disease, an alternative testing strategy is necessary. In this study, we compared NGS and IHC to determine the performance characteristics of pan-Trk and TrkA antibodies as a marker of *NTRK* rearrangements in pediatric mesenchymal tumors.

Conventional cytogenetic/molecular assays (FISH or RT-PCR) have been considered the gold standard for confirming a diagnosis of infantile fibrosarcoma/congenital mesoblastic nephroma; however, these tests failed to identify the classic *ETV6-NTRK3* fusion in 4 cases in which this fusion was later detected by NGS. Thus, while a positive result by traditional molecular/cytogenetic assays are specific for a gene rearrangement, false negative results may occur more commonly than generally thought. Church et al⁶ also described recurrent *EML4-NTRK3* fusions in a subset of infantile fibrosarcomas, and suggested expanding molecular testing for cases in which *ETV6* testing is negative.

The gold standard for identification of variant *NTRK* rearrangements is sequencing, either by DNA or RNA approaches; however, there are significant limitations to the routine use of these methods. Perhaps most important clinically, these tests are expensive, not available at many institutions, are often not covered by insurance, and have a long-turnaround time (often ≥ 2 wk). Both also require relatively large volumes of material (typically 5 to 10, 10- μ m-thick sections of formalin-fixed paraffin-embedded material). In addition, DNA-based panels may only include select introns rather than

the entire gene due to size/space constraints, and the presence of repetitive sequences may prevent tiling of the entire intron. While RNA-based approaches are not restricted to specific introns, they are still limited by the test design as well as the quantity and quality of extracted RNA.

Several studies describe the presence of pan-Trk or TrkA protein expression by IHC in *NTRK*-rearranged tumors. Positive immunostaining for TrkA has been described in Spitz nevi and soft tissue tumors,^{7,15,16} while pan-Trk was recently described as a reliable marker for (predominantly adult) *NTRK*-rearranged tumors, agnostic

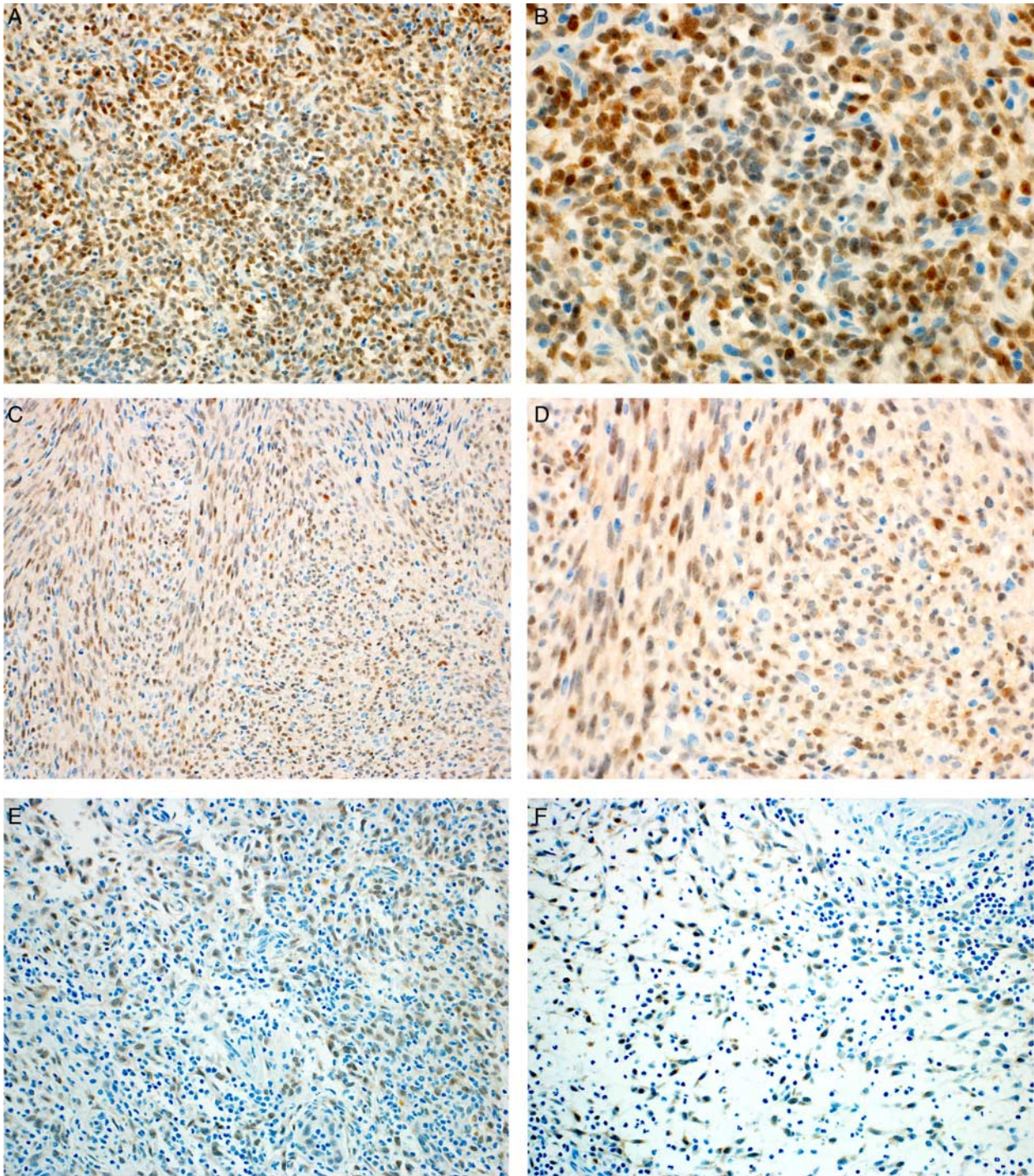


FIGURE 4. *NTRK3* rearrangement. Nuclear staining in *ETV6-NTRK3*-rearranged tumors ranged from strong (case 16: A, B) to moderate (case 17: C, D) to weak (case 18: E, F).

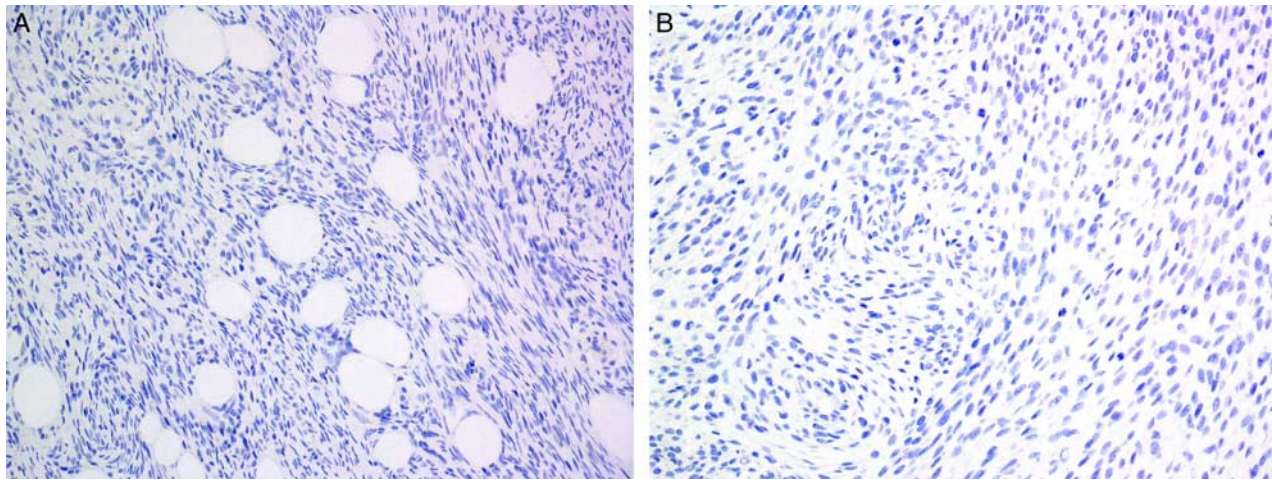


FIGURE 5. Pan-Trk IHC was negative in non-*NTRK*-rearranged cases; (A) dermatofibrosarcoma protuberans (case 1: pan-Trk) and (B) malignant peripheral nerve sheath tumor (case 20: pan-Trk).

of tumor type.¹⁷ However, this latter study included only 2 soft tissue tumors. Our series represents the largest study of Trk IHC in pediatric mesenchymal tumors.

Our study confirms pan-Trk IHC to be an excellent tool for identifying *NTRK*-rearranged mesenchymal tumors in children, with superior performance characteristics as compared with the TrkA antibody. The sensitivity of pan-Trk IHC as a surrogate marker of *NTRK* fusion status was 96.7%, similar to that demonstrated by Hechtman et al¹⁷ a single false negative *ETV6-NTRK3*-rearranged tumor was seen in both studies; although in our series this pan-Trk negative tumor showed diffuse, strong positivity for TrkA. In general, tumors harboring *NTRK3* rearrangements had much weaker staining for pan-Trk than tumors with *NTRK1/NTRK2* rearrangements. This differential expression, as well as the presence of nuclear staining in *NTRK3*-rearranged tumors, may be useful for directing subsequent molecular testing strategies. We did not observe the cytoplasmic or nuclear membrane patterns of staining previously described with *TPM3-NTRK1* or *LMNA-NTRK1* fusions. It is unclear if this represents a difference in expression patterns for sarcomas versus carcinomas, or if this reflects more general differences in the staining platforms.

Although Hechtman and colleagues showed 100% specificity of pan-Trk staining, we observed a single low-grade spindle cell lesion, NOS with weak but diffuse cytoplasmic pan-Trk staining that lacked an identifiable rearrangement by NGS. It is possible that an *NTRK* rearrangement or other alteration was missed given the limitations of a DNA assay, but a diagnostic alteration has not yet been found in this tumor. In addition, in 1 case there was partial low-level amplification of *NTRK1* exons 7 to 17 downstream of an apparent breakpoint in intron 6, but without a clear fusion partner identified. Both of these cases showed diffuse but weak, cytoplasmic expression of pan-Trk, without nuclear staining.

On the basis of our data, IHC appears to be a very useful tool in the identification of *NTRK* rearrangements

in pediatric mesenchymal tumors. We propose 1 possible algorithm for using pan-Trk IHC as a surrogate marker for *NTRK* rearrangements: moderate to strong diffuse cytoplasmic pan-Trk IHC staining can be considered diagnostic of *NTRK1/NTRK2* fusions and nuclear pan-Trk IHC can be considered a diagnostic surrogate of *NTRK3* fusions. For tumors with only weak cytoplasmic expression of pan-Trk, an *NTRK* fusion should be confirmed by other molecular/cytogenetic methods to ensure that a fusion is present in patients being considered for targeted therapeutic agents.

The field of molecular diagnostics is changing rapidly; however, IHC remains an invaluable tool for the practicing pathologist. In contrast to NGS methods, IHC is cheaper, more widely available, has a rapid turn around time (typically within 24 h), uses less tissue, and offers the advantage of direct histologic correlation. Our results indicate that pan-Trk IHC is an excellent diagnostic marker for *NTRK* rearrangements in pediatric mesenchymal tumors. We propose that IHC be used alone or as an adjunct to directed molecular testing in this clinical setting.

REFERENCES

- Amatu A, Sartore-Bianchi A, Siena S. NTRK gene fusions as novel targets of cancer therapy across multiple tumor types. *ESMO Open*. 2016;1:1–9.
- Knezevich SR, McFadden D, Tao W, et al. A novel *ETV6-NTRK3* gene fusion in congenital fibrosarcoma. *Nat Genet*. 1998;18:184–187.
- Rubin BP, Chen CJ, Morgan TW, et al. Congenital mesoblastic nephroma t(12;15) is associated with *ETV6-NTRK3* gene fusion: cytogenetic and molecular relationship to congenital (infantile) fibrosarcoma. *Am J Pathol*. 1998;153:1451–1458.
- Pavlick D, Schrock AB, Malicki D, et al. Identification of NTRK fusions in pediatric mesenchymal tumors. *Pediatr Blood Cancer*. 2017;64:e26433.
- Davis JL, Lockwood CM, Albert CM, et al. Infantile NTRK-associated Mesenchymal Tumors. *Pediatr Dev Pathol*. 2018;21:68–78.
- Church AJ, Calicchio ML, Nardi V, et al. Recurrent *EML4-NTRK3* fusions in infantile fibrosarcoma and congenital mesoblastic nephroma suggest a revised testing strategy. *Mod Pathol*. 2018;31:463–473.

7. Agaram NP, Zhang L, Sung YS, et al. Recurrent NTRK1 gene fusions define a novel subset of locally aggressive lipofibromatosis-like neural tumors. *Am J Surg Pathol*. 2016;40:1407–1416.
8. Haller F, Knopf J, Ackermann A, et al. Paediatric and adult soft tissue sarcomas with NTRK1 gene fusions: a subset of spindle cell sarcomas unified by a prominent myopericytic/haemangiopericytic pattern. *J Pathol*. 2016;238:700–710.
9. Nagasubramanian R, Wei J, Gordon P, et al. Infantile fibrosarcoma with NTRK3-ETV6 fusion successfully treated with the tropomyosin-related kinase inhibitor LOXO-101. *Pediatr Blood Cancer*. 2016;63:1468–1470.
10. Laetsch T, Nagasubramanian R, Casanova M. Targeting NTRK fusions for the treatment of congenital mesoblastic nephroma. *Pediatr Blood Cancer*. 2018;65:e26593.
11. Parikh AR, Corcoran RB. Fast-TRKing drug development for rare molecular targets. *Cancer Discov*. 2017;7:934–936.
12. Drilon A, Siena S, Ou SI, et al. Safety and antitumor activity of the multitargeted pan-Trk, ROS1, and ALK inhibitor Entrectinib: Combined results from two Phase 1 trials (ALKA-372-001 and STARTRK-1). *Cancer Discov*. 2017;7:400–409.
13. Laetsch TW, DuBois SG, Mascarenhas L, et al. Larotrectinib for paediatric solid tumours harbouring NTRK gene fusions: phase 1 results from a multicentre, open-label, phase 1/2 study. *Lancet Oncol* 2018. [Epub March 29, 2018].
14. Drilon A, Laetsch TW, Kummar S, et al. Efficacy of Larotrectinib in TRK fusion-positive cancers in adults and children. *N Engl J Med*. 2018;378:731–739.
15. Wiesner T, He J, Yelensky R, et al. Kinase fusions are frequent in Spitz tumors and spitzoid melanomas. *Nat Commun*. 2014;5:3116.
16. Lee CY, Sholl LM, Zhang B, et al. Atypical spitzoid neoplasms in childhood: a molecular and outcome study. *Am J Dermatopathol*. 2017;39:181–186.
17. Hechtman JF, Benayed R, Hyman DM, et al. Pan-Trk immunohistochemistry is an efficient and reliable screen for the detection of NTRK fusions. *Am J Surg Pathol*. 2017;41:1547–1551.